**Title Page**

**Title:** Cholinergic modulation of stimulus-specific adaptation in the inferior colliculus

**Abbreviated title:** Cholinergic modulation of auditory SSA

**Authors:** Yaneri A. Ayala[1], Manuel S. Malmierca[1,2]

**Affiliations:**

[1]Auditory Neuroscience Laboratory. Institute of Neuroscience of Castilla Y León, University of Salamanca, C/Pintor Fernando Gallego, 1, 37007 Salamanca, Spain.

[2] Department of Cell Biology and Pathology, Faculty of Medicine, University of Salamanca, Campus Miguel de Unamuno, 37007 Salamanca, Spain.

**Keywords**: acetylcholine, SSA, auditory, attention, neuromodulators, micrioiontophoresis

**Author Contribution**

M.S.M. and Y.A.A. designed the experiments, Y.A.A. performed the electrophysiological experiments and data analysis, Y.A.A. and M.S.M. wrote the manuscript.

**Corresponding author:**

Manuel S. Malmierca

Department of Cell Biology and Pathology, Faculty of Medicine, University of Salamanca, Campus Miguel de Unamuno, 37007 Salamanca, Spain. Tel: +34 923 294 500, ext. 5333. Fax: +34 923 294 750. e-mail: msm@usal.es

**Number of pages:** 47

**Number of figures:** 6

**Number of words for Abstract**: 206; **Introduction**: 453; **Discussion:** 1542.

**Acknowledgements**

We thank Drs. Nell Cant, Raju Metherate and Adrian Rees, for their comments on a previous version of the manuscript and for their constructive criticisms. This project was funded by the MINECO grant BFU201343608-P and the JCYL grant SA343U14 to M.S.M. Y.A.A. held a CONACyT (216106) and a SEP fellowship. The authors declare no competing financial interests.

**Abstract**

Neural encoding of an ever-changing acoustic environment is a complex and demanding task that may depend on modulation by the animal´s attention. Some neurons of the inferior colliculus (IC) exhibit 'stimulus-specific adaptation (SSA)', *i.e.*, a decrease in their response to a repetitive sound but not to a rare one. Previous studies have demonstrated that acetylcholine (ACh) alters the frequency response areas of auditory neurons and therefore is important in the encoding of spectral information. Here, we address how microiontophretic application of ACh modulates SSA in the IC. We found that ACh decreased SSA in IC neurons by increasing the response to the repetititve tone. This effect was mainly mediated by muscarinic receptors. The strength of the cholinergic modulation depended on the baseline SSA level, exerting its greatest effect on neurons with intermediate SSA responses across cortical IC subdivisions. Our data demonstrates that ACh alters the sensitivity of partially-adapting IC neurons by switching neural discriminability to a more linear transmission of sounds. This change serves to increase ascending sensory-evoked afferent activity propagated through the thalamus *en route* to the cortex. Our results provide empirical support for the notion that high ACh levels may enhance attention to the environment, making neural circuits more responsive to external sensory stimuli.

## Introduction

Neural encoding of an ever-changing acoustic environment is a complex and demanding task that may depend on modulation by an animal´s attention or by the demands of ongoing activity (Sarter et al., 2005; Thiel and Fink, 2008; Edeline, 2012). Neural mechanisms for detecting sensory changes engage a distributed network of neural circuits that are sensitive to stimulation history (Ranganath and Rainer, 2003; Grimm and Escera, 2012).

In the auditory brain, neurons that specifically decrease their response to a repeated sound but resume their firing when deviant stimuli are presented are found in the primary auditory cortex (AC, Ulanovsky et al., 2003; von der Behrens et al., 2009), auditory thalamus (Antunes et al., 2010) and inferior colliculus (IC, Perez-Gonzalez, 2005; Malmierca et al., 2009). This differential response to repeated versus rare sounds is referred to as ‘stimulus-specific adaptation' (SSA) and might reflect a special type of short-term plasticity that transiently modulates neural responsiveness in an activity-dependent manner (Jääskeläinen et al., 2007; Nelken, 2014). SSA may contribute to the upstream encoding of mismatch signals to repeated and deviant sounds observed at larger spatial and temporal scales in electroencephalographic studies (Nelken and Ulanovsky, 2007; Escera and Malmierca 2014; Malmierca et al., 2014). In humans, the encoding of repeated and rare sounds is affected by top-down processing (Todorovic et al., 2011) and by the application of modulatory substances, such as cholinergic compounds, that are known to vary across vigilance and cognitive states (Knott et al., 2014; Moran et al., 2013; Grupe et al., 2013).

An augmentation of aceytlycholine (ACh) release occurs during attention-demanding tasks (Himmelheber et al., 2000; Passetti et al., 2000). The increase in ACh

52 modifies circuit dynamics in response to internal and external inputs (Sarter et al., 2005;
53 Hasselmo and McGaurghy, 2004; Picciotto et al., 2012). It has been suggested that
54 cholinergic modulation may shift brain activity from a discrimination mode to a detection
55 mode, thus favoring the encoding of ongoing stimulation (Sarter et al., 2005; Hasselmo and
56 McGaughy, 2004; Jääskeläinen et al., 2007). In the AC, ACh enhances responses to
57 afferent sensory input while decreasing intracortical processing (Metherate and Ashe, 1993;
58 Hsieh et al., 2000). Moreover, previous studies have demonstrated that cholinergic
59 modulation alters frequency response areas of auditory neurons and therefore is important
60 in the encoding of spectral representation (Ashe et al., 1989; Metherate and Weinberger,
61 1989, 1990; Metherate et al., 1990; Ma and Suga, 2005; IC: Ji et al., 2001).

62 The main goal of the present study was to analyse what role, if any, ACh plays in
63 generation or modulation of SSA. We employed microiontophretic application of ACh to
64 address how ACh affects the responses of IC neurons that exhibit SSA. Preliminary reports
65 have been presented elsewhere (Ayala and Malmierca, 2014, 2015).

66

## Material and methods

### *Subjects and surgical procedures*

Experiments were performed on 44 adult female rats (*Rattus norvegicus*, Rj: Long-Evans) with body weights ranging from 180–333 g (median ± SEM: 210 ± 0.76 g). All surgical, recording and histological procedures were conducted at the University of Salamanca, Spain. The experimental protocols were approved by Animal Care Committees of the University of Salamanca and followed the standards of the European Union (Directive 2010/63/EU) for the use of animals in neuroscience research. Detailed procedures are given elsewhere (Malmierca et al., 2003; Malmierca et al., 2009; Perez-Gonzalez et al., 2012). Anesthesia was induced using a mixture of ketamine chlorohydrate (30 mg/kg, I.M., Imalgene 1000, Rhone Méreuse, Lyon, France) and xylazine chlorohydrate (5 mg/ Kg, Rompun, Bayer, Leverkusen, Germany). Body temperature was monitored with a rectal probe and maintained at 38 ± 1ºC with a thermostatically controlled electric blanket. The trachea was cannulated and atropine sulphate (0.05 mg/kg, s.c., Braun, Barcelona, Spain) was administered to reduce bronchial secretions. The animals were connected to aventilator (SAR-830/P) and expired $CO_2$ was monitored using a capnograph (Capstar-100). A craniotomy was made in the caudal part of the left and right parietal bone, exposing the cerebral cortex, in order to gain access to the IC. To perform electrophysiological recordings from IC neurons, anesthesia was maintained with an initial i.p. injection of urethane (750 mg/kg, Sigma-Aldrich Corp., St Louis, MO, USA) and with booster doses of one-third of the initial amount.

### *Acoustic delivery and electrophysiological recording*

89 Prior to surgery, auditory brainstem responses (ABRs) to clicks (100 μs, 10 Hz rate)
90 delivered in 10 dB SPL ascending steps from 10 to 90 dB SPL were obtained to check that
91 the animal had normal hearing with thresholds lower or at 30 dB SPL. ABR recordings
92 were performed inside a sound-attenuated room, using a closed-field sound delivery system
93 and a real-time signal processing system (Tucker-Davis Technologies System 3, Alachua,
94 Florida, USA). Subcutaneous needle electrodes placed at the vertex (active electrode), the
95 mastoid ipsilateral to the stimulated ear (reference electrode) and the mastoid contralateral
96 to the stimulated ear (ground electrode) were used for the recordings. Evoked potentials
97 were averaged from 500 presentations, and the final signal was filtered with a 500-Hz high-
98 pass filter and a 3000-Hz low-pass filter with hearing thresholds determined visually.
99 Afterwards, the animal was placed in a stereotaxic frame in which the ear bars were
100 replaced by a hollow speculum that accommodated a sound delivery system (Rees, 1990)
101 using two electrostatic loudspeakers (TDT-EC1). Search stimuli were pure tones or white
102 noise driven by a TDT System 2 (TDT, Tucker-Davis Technologies, Florida, USA) that
103 was controlled by custom software for stimulus generation and on-line data visualization
104 (Faure et al., 2003; Pérez-González et al., 2005; Malmierca et al., 2008). Action potentials
105 were recorded with a TDT BIOAMP amplifier, the ×10 output of which was further
106 amplified and bandpass-filtered (TDT PC1; fc: 0.5–3 kHz) before passing through a spike
107 discriminator (TDT SD1). Spike times were logged at one microsecond resolution on a
108 computer by feeding the output of the spike discriminator into an event timer (TDT ET1)
109 synchronized to a timing generator (TDT TG6). Extracellular single-unit responses were
110 recorded in the left and/or right IC of each animal to contralateral stimulation. The IC was
111 approached from 20° relative to the frontal plane so that the recording electrode moved

caudal and ventral during the penetration. The electrode was lowered into the brain with a piezoelectric microdrive (Burleigh 6000 ULN) mounted on a stereotaxic manipulator to a depth of 3.5–5 mm where acoustically driven responses were found. After a neuron was isolated, pure tone stimuli with a duration of 75 ms (5 ms rise/fall time) were delivered to obtain the monaural frequency response area (FRA), *i.e.,* the combination of frequencies and intensities capable of evoking a suprathreshold response. To do this, 5 stimulus repetitions at each frequency (from 0.5 to 40 kHz, in 20–25 logarithmic steps) and intensity step (steps of 10 dB, from 0 to 80 dB SPL) were presented randomly at a repetition rate of 4 Hz.

*Stimulus presentation paradigm*

Pure tones (75 ms, 5 ms rise/fall time) were presented in an oddball paradigm similar to that used to record mismatch negativity responses in human studies (Näätänen, 1992) and more recently in animal studies of SSA (Ulanovsky et al., 2003; Malmierca, et al., 2009, von der Behrens et al., 2010). Briefly, this paradigm consists of a flip-flop design employing two pure tones at two different frequencies (f1 and f2), both of which elicited similar firing rates and response patterns at a level of 10–40 dB SPL above threshold within the neural FRA. For most of the neurons (64%), the f1 and f2 tones were located around the characteristic frequency (CF, the sound frequency that produces a response at the lowest stimulus level) while the rest of the frequency pairs were both either lower (23%) or higher (13%) than the CF. The frequency separations (Δf) between f1 and f2 varied between 0.14 octaves and 0.53 octaves. A train of 300 or 400 stimulus presentations containing both frequencies was delivered in two different sequences (sequence 1 and 2). The repetition rate of the train of stimuli was 4 Hz, as this has been previously demonstrated to elicit SSA in

IC neurons of the rat (Malmierca et al., 2009; Ayala and Malmierca, 2013). In sequence 1, the f1 frequency was presented as the standard tone with a high probability of occurrence (90%) within the sequence. Interspersed randomly among the standard stimuli were the f2 frequency-deviant stimuli (10% probability). After the sequence 1 data set was obtained, the relative probabilities of the two stimuli were reversed, with f2 as the standard and f1 as the deviant in sequence 2. The responses to the standard and deviant stimuli were normalized to spikes per stimulus, to account for the different number of presentations in each condition.

*Electrodes and iontophoresis*

A tungsten electrode (1–2.5 MΩ, Merrill and Ainsworth, 1972) was used to record single-neuron activity. It was attached to a multibarrel borosilicate glass pipette that carried drugs to be delivered in the vicinity of the recorded neuron. The tip of the recording electrode protruded 15–25 μm from the pipette tip. The glass pipette consisted of five barrels in H-configuration (World Precision Instruments, 5B120F-4) with the tip broken to a diameter of 20–30 μm. The center barrel was filled with saline for current compensation (165 mM NaCl), while the others were filled with 1 M ACh chloride (Sigma, A6625), 0.5 M scopolamine hydrobromide (Sigma, S0929) or 0.5 M mecamylamine hydrochloride (Tocris, 2843). The drugs were dissolved in distilled water and their pH adjusted to 4–4.2. ACh chloride acts at both muscarinic and nicotinic receptors while the scopolamine and mecamylamine are non-selective antagonists of muscarinic and nicotinic receptors, respectively. These compounds have been used previously in the mammalian IC (Farley et al., 1983; Habbicht and Vater, 1996). The drugs were retained in the pipette with a –15 nA current and were ejected, when required, typically using 30–40 nA currents (Neurophore

158 BH-2 System, Harvard Apparatus). The duration of the drug ejection usually lasted 15–25
159 min but could be extended when no visual effect was observed in order to ensure the
160 absence of effect. After the drug injection, we repeated the stimulation protocol until we
161 observed recovery of firing.

162 *Verification of the recording sites*

163 Once the electrophysiological recordings were completed, electrolytic lesions (10–20 μA
164 for 15 s) were applied for subsequent histological verification of the recording sites in 24 of
165 the 44 animals. Brains were fixed using a mixture of 1% paraformaldehyde and 1%
166 glutaraldehyde diluted in 0.4 M phosphate buffer saline (0.5% NaNO3 in PBS). After
167 fixation, tissue was cryoprotected in 30% sucrose and sectioned in the coronal or sagital
168 plane at a thickness of 50 μm on a freezing microtome. Slices were stained with 0.1%
169 cresyl violet to facilitate identification of cytoarchitectural boundaries. The recorded units
170 were assigned to one of the four main subdivisions of the IC (rostral, lateral and dorsal
171 cortices or central nucleus, Loftus et al., 2008; Ayala et al., 2015) using as reference the
172 standard sections from a rat brain atlas (Paxinos and Watson, 2005).

173 *Analysis of neural responses*

174 For each neuron, the degree of SSA was quantified by the Common-SSA Index (CSI) and
175 the Frequency-Specific SSA Index (SI) reported previously (Ulanovsky et al., 2003;
176 Malmierca et al., 2009; von der Behrens et al., 2009; Richardson et al., 2013). Both SSA
177 indices reflect the normalized difference between the neural response to the deviant
178 stimulus and the response to the standard, averaging (CSI) or quantifying separately (SI)
179 the responses to f1 and f2. The CSI is defined as

$$CSI = [d(f1) + d(f2) - s(f1) - s(f2)] / [d(f1) + d(f2) + s(f1) + s(f2)]$$

where d(f) and s(f) are responses to each frequency f1 or f2 when they were the deviant (d) or standard (s) stimulus, respectively. The SI was separately calculated for each frequency and it is defined as

$$SI(fi) = [d(fi) - s(fi)] / [d(fi) + s(fi)]$$

where i = 1 or 2. Positive CSI and SI values indicate that the neurons responded more strongly to the frequencies when they were deviant compared to when they were standard. A CSI value of 0.1 was used as cutoff between neurons that exhibited or lacked SSA since it has been previously demonstrated that CSIs < 0.1 are not statistically different from zero and are due to random fluctuations in spike counts (Ayala et al., 2013).

To characterize the time course of adaptation, we averaged the response of all neurons to the standard tone (mean spikes per trial). This was done trial by trial for the total of stimulus presentations under the oddball paradigm. The mean response was plotted at their original trial-long time scale. Then, we performed a nonlinear least-square fit to this population mean curve to find the best-fitting double exponential function as follows:

$$f(t) = A_{ss} + A_r \cdot e^{-t/\tau(r)} + A_s \cdot e^{-t/\tau(s)},$$

where $A_{ss}$, $A_r$ and $A_s$ are the magnitudes of the steady state, and the rapid and slow components, respectively, and $\tau_r$ and $\tau_s$ are the time constants of the rapid and slow components (see details in Perez-Gonzalez et al., 2012).

The CF and threshold of each neuron was identified. The monotonicity index (MI = spike count at 80 dB SPL / maximum spike count) that refers to the degree of reduced

spiking at higher intensities was calculated from the FRA measure at the CF (Watkins and Barbour, 2011). Monotonic responses were those with a MI > 0.75. Finally, we measured the sharpness of the FRA by calculating the Q-value at 10 above the threshold as in previous studies (Hernandez et al., 2005; Malmierca et al., 2009; Duque et al., 2012; Ayala et al., 2013). The $Q_{10}$-value was calculated as the CF divided by the bandwidth which is the difference in kHz between the lower and upper frequencies of the FRA. To test for significant effects of the drugs on each individual neuron, the 95% confidence intervals (C.Is.) for the baseline CSI were calculated using the bootstrapping method (1000 repetitions). The limits of 95% CIs were calculated using the 2.5 and 97.5 percentiles of the CSI bootstrap distribution. An effect of the drug was considered to be significant when the CSI value obtained under the injection condition was larger or smaller than the high or low 95% C.I., respectively.

To study the contribution of spontaneous activity on the SSA, we again calculated the SSA indices from the evoked activity but with subtracted spontaneous activity bin by bin (evoked activity minus spontaneous activity in spikes/s). Spontaneous activity was estimated within a 50 ms window before each tone presentation in the oddball paradigm as described previously (Duque and Malmierca, 2014). Unless otherwise stated, results are presented as median ± SEM. To test for significant differences among medians, distributions across baseline, drug application and recovery conditions we performed the Friedman Repeated Measures Analysis of Variance on Ranks. Post hoc comparisons were performed following Dunn's method and a $p < 0.05$ was considered statistically significant. To measure the strength of association between variables we used the Spearman Rank Order Correlation Coefficient. Analyses and figures were executed using SigmaPlot

224 Version 11 (Systat Software, Inc., Chicago, IL, USA) and Matlab 13 (MathWorks, Inc.,
225 Natick, MA, USA).

226

## Results

To explore the influence of cholinergic neuromodulation on SSA in the IC of the rat, we recorded the responses of 152 well-isolated single neurons to an oddball paradigm before, during and after microiontophoretic application of ACh (n = 105), scopolamine (n = 19), and mecamylamine (n = 28).

### The strength of the ACh effect depends on the baseline SSA level

The recorded neurons had different temporal response patterns and exhibited (82 %) or lacked SSA (18 %). Three example neurons are shown in Figure 1. The first neuron (Fig. 1A) responded with sustained firing of similar strength to both the deviant and standard tones across all the tone presentations; therefore it lacks SSA ($CSI_{baseline}$ = 0.076). Microiontophoretic application of ACh did not change either the temporal response pattern or the ratio between the responses to the standard and deviant sound as estimated by its CSI = 0.072 (Bootstrapping, 95% C.I., Fig. 1A,B). Figure 1C illustrates another neuron that showed an onset response type and a high level of SSA as depicted by its CSI (0.974). It was also unaffected by ACh, even after a long period of application (more than 2 hours; Fig. 1C,D). In contrast, Figure 1E,F depicts the response of a third neuron, with an intermediate CSI value (0.732), that was strongly affected by ACh. In this neuron, the firing response increased (Fig. 1E) and the CSI (0.41, Fig. 1F) decreased significantly but returned to baseline values during recovery (Fig. 1F).

Our data (n = 105) contains a wide range of CSI values from −0.063 to 0.994 (Fig. 2A) and thus includes neurons that lack or exhibit different levels of SSA. Across the entire sample, the most remarkable finding was that ACh differentially affected only a subset of

IC neurons (54 out of 105, Bootstrapping, 95% C.I.), mainly by decreasing their CSI (36 out 54). The majority of neurons with intermediate CSI values were sensitive to the ACh application ($0.1 < CSI < 0.9$, 43 out 62), whereas most of the neurons that exhibited low ($CSI \leq 0.1$; 15 out 19) or high ($CSI \geq 0.9$, 17 out 24) values were unaffected by ACh (Fig. 2A). The different baseline CSI values of our sample of neurons were fitted by a Sigmoidal curve ($r^2 = 0.99$, $p < 0.0001$, Fig. 2B, gray line). We found that the magnitude of the absolute change exerted by ACh on the CSI followed a Gaussian distribution ($r^2 = 0.44$, $p < 0001$, Fig. 2B, black line). The tails of the Gaussian curve correspond to the weak or absent effect exerted on neurons with low or extremely high CSI values, and the peak corresponds to the maximum effect exerted on neurons with intermediate CSI values. These results indicate a distinct dependence of the strength of the ACh effect on the baseline CSI. This dependence was also evident in the normalized responses to each frequency (f1 or f2) estimated by the SIs (Fig. 2C). There was no difference between the absolute change on SI1 and SI2 (Mann-Whitney Rank Sum Test, $p = 0.696$, $T = 11250$, $n = 105$), indicating that ACh affected both frequencies similarly. Also, the absolute change exerted by ACh on the CSI correlated with the changes elicited on SI1 (Spearman´s coefficient: 0.63, $p = < 0.001$, $n = 210$) and SI2 (coefficient: 0.59, $p < 0.001$, $n = 210$, Fig. 2D). The magnitude of change on SI was higher for the group of neurons with $0.1 < CSI < 0.9$ while for the neurons with $CSI < 0.1$ and $CSI > 0.9$, this magnitude was similar (Kruskal-Wallis One Way ANOVA, $p < 0.001$, $H = 38.759$, Dunn´s Method, $p < 0.05$, $n = 210$). Hence, we can safely conclude that ACh decreased both the CSI and SI at the population level. The CSI decreased from $0.57 \pm 0.034$ to $0.452 \pm 0.035$ (Friedman test, $p = 0.01$, $Xi^2 = 8.9$, $n = 105$) and the SI from $0.574 \pm 0.025$ to $0.443 \pm 0.025$ (Friedman test, $p = 0.009$, $Xi^2 = 9.36$, $n = 210$, Fig. 2E). The

recovery values for most neurons were virtually identical to the baseline cases ($CSI_{rec}$ = 0.522 ± 0.036, $SI_{rec}$ = 0.535 ± 0.027). Twelve neurons that were manipulated with ACh (11% of the sample) were lost before the full recovery (crosses in Figure 2A). Nevertheless, those 12 neurons were distributed along the whole spectrum of CSI values in the sample and followed the same trend. They were similarly affected by ACh as other neurons with a similar baseline CSI (Figure 2A, crosses). Furthermore, ACh increased the spontaneous rate (from 0.17 ± 0.49 to 0.28 ± 0.97 spikes per second) of those IC neurons with partial levels of CSI ($0.1 < CSI < 0.9$, Wilcoxon Signed Rank Test, W = 476, Z-statics = 2.441, p = 0.015, n = 62) but did not affect the spontaneous discharge of those with low ($CSI \leq 0.1$, p = 0.232, n = 19) or high CSI values ($CSI \geq 0.9$, p = 0.375, n = 24). Based on this result we subtracted the spontaneous rate from the evoked response and recalculated the SSA indices of all neurons in order to validate that the changes we observed were due to an ACh effect on the driven responses. Under this manipulation, the SSA indices across the baseline, ACh and recovery condition were increased, but the ACh still decreased the CSI (Friedman test, p = 0.01, $Xi^2$ = 9.31, n = 210) and SI (Friedman test, p = 0.002, $Xi^2$ = 12.04, n = 210, Fig. 2E) indicating a genuine cholinergic effect on the evoked responses.

**Acetylcholine differentially modulates the responses to deviant- and standard tones**

In terms of spike count (spikes per trial), positive CSI values reflect smaller spike count to the standard tone than to the deviant one. In agreement with this, the spike count to the standard sound was negatively correlated with the CSI (Spearman´s coefficient = −0.932, p < 0.001, n = 105), while the response to the deviant sound elicited a weaker correlation (−0.512, p < 0.001, n = 105). The firing rate of the neural responses was significantly affected by the ACh (Friedman test, $Xi^2$ = 405.112, p < 0.001). The post hoc analysis

295 indicated that the spike count to the deviant was higher (1.05 ± 0.106 spikes per trial) than
296 to the standard tone (0.262 ± 0.102 spikes per trial) in the baseline condition as expected,
297 since our sample was biased to positive CSI values ($p < 0.05$). ACh increased the spike
298 count to both the deviant and standard tones to 1.188 ± 0.133 and 0.421 ± 0.128 spikes per
299 trial, respectively ($p < 0.05$) without eliminating the difference between them (Fig. 3A,B).
300 In the recovery condition, the ACh effect on the neural firing was completely abolished and
301 the response decreased to baseline values; 1.125 ± 0.122 and 0.246 ± 0.116 for the deviant
302 and standard tone, respectively ($p < 0.05$). Since ACh did not affect all neurons with
303 different CSI values equally, we explored the change in the spike count of those partially
304 adapting neurons whose CSI was significantly changed by ACh application ($n = 43$). Most
305 notably, for this group of neurons we found that ACh only increased the response to the
306 standard tone (Friedman test, $Xi^2 = 204.847$, $p < 0.001$, Fig. 3C,D). Moreover, the
307 differential effect exerted by ACh on the response to the standard stimulus was also
308 apparent for all neurons with a significant change in their CSI ($n = 54$, Friedman test, $Xi^2 =$
309 232.583, $p < 0.001$).

310 We analyzed the effect of ACh on the time course of the response to the standard
311 tone for those partially adapting neurons with a significant change in their CSI. The
312 dynamics of the response to the standard tone was fit well by a double exponential function
313 under the baseline ($r^2 = 0.7871$) and ACh ($r^2 = 0.7767$) condition, displaying a rapid and a
314 slow decay as well as a steady-state component (Fig. 3E). ACh increased the response
315 during the steady-state component of the response from 0.6343 spikes per trial (95% C.Is.:
316 0.6246, 0.6441) to 0.9932 (0.9825, 1.004) (Fig. 3E) without affecting either the timing or
317 the magnitude of the fast (baseline: $\tau_r = 0.6165$ trial, $A_r = 4.973$ spikes per trial; ACh: $\tau_r =$

318 0.596, $A_r = 6.536$) and slow (baseline: $\tau_s = 29.15$, $A_s = 0.4969$; ACh: $\tau_s = 26.7$, $A_s = 0.5197$)
319 components of the adaptation.

320 The differential effect exerted by ACh on the response to the standard and deviant
321 tone was also reflected by the strength of correlation between the change in the CSI
322 ($CSI_{ACh} - CSI_{baseline}$) and spike count. The change in the CSI was correlated stronger with
323 the normalized change in the mean spiking response to f1 and f2 when presented as
324 standard ($r^2 = -0.7$, $p < 0.001$, $n = 105$) than with the change in the response to f1 and f2
325 when presented as deviant tone ($r^2 = -0.3$, $p < 0.001$, Fig. 3F,G). We explored the effect of
326 ACh on the first spike latency (FSL) of the response to the deviant and standard tone. As
327 expected from previous IC studies (Malmierca et al., 2009), the FSL of the deviant (15.55 ±
328 0.43 ms) was shorter than the FSL of the standard response (16.2 ± 0.67 ms, $p < 0.05$) in
329 the baseline condition. ACh did not affect the FSL; the response latency to the deviant tone
330 remained shorter during the injection (deviant: 15.2 ± 0.46 ms; standard: 15.87 ± 0.64 ms)
331 and recovery conditions (deviant: 15.61 ± 0.54 ms; standard: 15.71 ± 0.75 ms) (Friedman
332 test $Xi^2 = 68.064$, $p < 0.001$).

333 Next, to assure that the lack of effect on the CSI we observed in some neurons was
334 not due to a failed iontophoretic release of ACh, we measured the CF, MI and threshold of
335 most of the neuronal FRAs (96 out 105) before and during the ACh application. We found
336 that the threshold was affected (Wilcoxon Signed Rank Test, $W = -747$, Z-statics = −4.037,
337 $p < 0.001$, $n = 96$) while the CF (Wilcoxon Signed Rank Test, $W = -168$, Z-statics =
338 −0.836, $p = 0.406$, $n = 96$) and MI (Wilcoxon Signed Rank Test, $W = 211$, Z-statics =
339 0.934, $p = 0.353$, $n = 96$) remained unchanged by ACh. Moreover, the threshold of both
340 groups of neurons, *i.e.*, neurons with significant change in their CSI (Wilcoxon Signed

Rank Test, W = −226, Z-statics = −2.973, p = 0.003, n = 50) as well as those whose CSI was unaffected by ACh (Wilcoxon Signed Rank Test, W = −158, Z-statics = −2.747, p = 0.006, n = 46) was lowered from 30 to 20 dB SPL. These results demonstrate that the differential effects elicited by ACh on the CSI were genuine and not an artifact.

**The effect of the ACh on SSA responses is mainly mediated by the mAChRs**

Two major classes of cholinergic receptors (muscarinic and nicotinic) are distributed throughout the IC (Morley and Kemp, 1981; Clarke et al., 1985; Kelly and Caspary, 2005). To examine whether the ACh effects described above are mediated by the muscarinic and/or nicotinic receptors, we recorded 47 additional neurons before, during and after the microiontophoretic application of their respective antagonists; *i.e.*, scopolamine and mecamylamine. The application of scopolamine affected the CSI of 15 out 19 neurons (Fig. 4A) while the mecamylamine affected 16 out 28 neurons (Fig, 4B, Bootstrapping, 95% C.I.). The majority of the significantly affected neurons showed an increase in their CSI under the blockade of the muscarinic (n = 12 out of 15, Fig. 4A) and nicotinic (n = 12 out of 16, Fig. 4B) receptors. The magnitude of the effect of both antagonists exhibited the same dependence on baseline CSI value as with ACh. The greatest changes elicited by the scopolamine and mecamylamine were on neurons with intermediate CSI values and the absolute changes followed a Gaussian distribution ($r^2 = 0.52$, $p = 0.003$ and $r^2 = 0.756$, $p < 0.0001$, respectively, Fig. 4A,B).

At the population level, only scopolamine significantly increased the CSI (Friedman test, $Xi^2 = 7$, $p = 0.03$, $n = 19$, Fig. 4C). Mecamylamine application did not significantly increase the CSI of the whole population (Friedman test, $Xi^2 = 1.52$, $p = 0.468$,

363 n = 28, Fig. 4D) neither for the group of neurons with intermediate CSI values that were
364 most affected at the single-neuron analysis (0.1 < CSI < 0.9) (Friedman test, $Xi^2 = 5.286$, p
365 = 0.071, n = 17). Likewise, the SI was affected by scopolamine (Friedman test, $Xi^2 = 7.357$,
366 p = 0.025, n = 38, Fig, 4E,F) but not by mecamylamine (Friedman test, p = 0.364, $Xi^2 =$
367 2.02, n = 56, Fig. 4E,G). The blockade of the cholinergic receptors decreased the response
368 only to the deviant tone (Friedman test, p < 0.001). The driving response changed from
369 1.171 ± 0.166 to 0.95 ± 0. 111 spikes per trial under the scopolamine injection (Friedman
370 test $Xi^2 = 66.375$, p < 0.001, Dunn´s Method, p < 0.05, n = 38) and from 1.283 ± 0.132 to
371 0.95 ± 0.139 spikes per trial (Friedman test $Xi^2 = 148.844$, p < 0.001, Dunn´s Method, p <
372 0.05, n = 56) under the mecamylamine application. Although the mean population response
373 to the standard tone was not significantly affected, we observed a clear change in the
374 temporal course of adaptation elicited by the muscarinic and nicotinic blockade (Fig. 4H,I).
375 The standard responses of those neurons with intermediate (0.1 < CSI < 0.9) and significant
376 change in their CSI under the scopolamine ($r^2 = 0.66$) and mecamylmine application ($r^2 =$
377 0.61) were fitted by the double exponential function previously described for ACh. We
378 found that scopolamine caused a greater decrease in the response during the steady-state in
379 comparison with mecamylamine effect. The response showed a 53% change from 0.6084
380 spikes per trial (C.I. 95%: 0.59, 0.6268) to 0.2857 (0.2733, 0.2981) with application of
381 scopolamine (Fig. 4H) while the change was only 29%, from 0.5043 (0.487, 0.5216) to
382 0.3565 (0.3448, 0.3682) with mecamylamine application (Fig. 4I). The magnitude and
383 timing of the rapid and slow decay of the response to the standard were not affected by
384 cholinergic blockade.

385 **Anatomical and physiological correlates of the ACh effect**

We determined the location of the majority of the recorded neurons (64 out 105) across IC subdivisions. Most of the neurons were located in the RCIC (n = 34) and the remaining neurons were distributed in the LCIC (n = 17) and CNIC (n = 13). The baseline SSA was higher in the cortical subdivisions (RCIC: 0.62 ± 0.058; LCIC: 0.72 ± 0.076) than in the central nucleus (0.13 ± 0.069) (Kruskal-Wallis One Way ANOVA, H = 12.983, p = 0.002; Fig. 5A). Interestingly, the magnitude of change exerted on the CSI by ACh in RCIC and LCIC neurons followed the same Gaussian distribution as the whole population depicted in Figure 2B ($r^2 = 0.47$, $p < 0.0001$ and $r^2 = 0.47$, $p = 0.011$, respectively) (Fig. 5B) while the sample of neurons from the CNIC showed a weak effect that was not Gaussianly distributed (p = 1, Fig. 5C).

Finally, we wished to test whether any other response feature in addition to the baseline CSI correlates with the presence or absence of ACh effect on SSA. We found that the MI of the group of neurons whose CSI was affected by the ACh (1 ± 0.0229, n = 54) was slightly higher than the MI of the group of neurons with non-affected CSIs (0.929 ± 0.0322, n = 51) (Mann-Whitney Rank Sum Test, U-statics = 996.5, T = 2322.5, p = 0.037), but in both cases the MIs were monotonic. Neither group differed in other parameters such as the response duration (67.55 ± 3.466 and 42 ± 3.634 ms for affected and unaffected groups, respectively, Mann-Whitney Rank Sum Test, p =0.614), threshold (30 ± 1.879, 30 ± 2.008 dB SPL, p = 0.263), $Q_{10}$ (1.426 ± 0.123, 1.556 ± 1.204, p = 0.601) or CF (11.245 ± 1.026, 11.199 ± 0.998 kHz, p = 0.605). The CF (Spearman´s coefficient = 0.806, p = 0.003, Fig. 5D) as well as the response duration (Spearman´s coefficient = −0.612, p = 0.053, Fig. 5E) correlated with the CSI at the baseline condition, *i.e.* neurons with higher CSI are tuned to higher frequencies and have shorter response durations. Then, the median CF and

409 reponse duration of the group of unaffected neurons may have been averaged out
410 explaining the lack of difference between the group of neurons whose CSI was or not
411 affected by ACh.

412

## DISCUSSION

We have demonstrated that application of ACh decreases the SSA of IC neurons by increasing the response to the standard tone and that this effect is mainly mediated by muscarinic receptors. Moreover, we have found that the strength of the cholinergic modulation depends on the baseline SSA level, exerting its greatest effect on neurons with intermediate SSA responses. To the best of our knowledge, this is the first study demonstrating that auditory SSA is sensitive to cholinergic modulation.

A selective effect of ACh on frequency processing has been described in AC neurons. A repeated single-frequency stimulus simultaneously paired with the iontophoretic application of ACh produced a highly specific change in the response to the paired frequency rather than a general change in excitability (Metherate and Weinberger, 1989). The effect was mediated by muscarinic receptors. Similar mechanisms may underly the selective change in the response to the standard tone that we observed (Fig. 3C,D), since this tone was repeated many more times than the deviant tone under ACh application. The observed decrease in the adaptation to the standard tones agrees with diminished spike-frequency adaptation exerted by ACh in other sensory areas (Metherate et al., 1992; McCormick, 1993; Martin-Cortecero and Nunez, 2014). Likewise, ACh affected SSA mainly through the activation of the muscarinic rather than the nicotinic receptors (Fig. 4G-H). Muscarinic receptors are expressed both pre- and postsynaptically so they can alter the excitability of the neurons as well as the release probability of other neurotransmitters (Zhang et al., 2002; Thiele, 2013). In the IC, at least two types of muscarinic receptors (M1- and M2-types) can functionally modify neural firing (Habbicht and Vater, 1996). Since we used a general antagonist for muscarinic receptors, we cannot discriminate

436 between the effects of the two muscarinic subtypes, but it is likely that most of the
437 excitatory effect exerted by ACh was mediated by the activation of the M1-type since
438 selective blockade of the M1 receptor mostly leads to inhibition whereas the opposite effect
439 occurs with selective blockade of the M2-type (Habbicht and Vater, 1996).

440 The excitatory effects elicited by ACh might be mediated through the regulation of
441 $K^+$ channels (McCormick and Prince, 1986; Krnjevic, 2004). The activation of the M1-type
442 receptor induces a reduction in hyperpolarizing potassium currents through the closure of
443 $K^+$ channels such as the slow after-hyperpolarization $K^+$ ($K_{sAHP}$) or the inward rectifying $K^+$
444 of type 2 (KIR2) which, in turn, reduces spike frequency adaptation and increases driven
445 and spontaneous activity (Cole and Nicoll, 1984; Krause and Pedarzani, 2000; Thiele,
446 2013). Changes in potassium conductance can act as an activity-dependent adaptation
447 mechanism (Sanchez-Vives et al., 2000a,b) that contributes to a significant fraction of
448 cortical auditory adaptation (Abolafia et al., 2011). For those reasons, $K^+$-mediated
449 adaptation has been proposed as a potential mechanism underlying SSA (Abolafia et al.,
450 2011; reviewed in Malmierca et al., 2014). ACh might also increase the tone-evoked
451 responsivity in IC by modulating the release of other neurotransmitters as reported in the
452 AC (Metherate, 2011) where the activation of cholinergic receptors decreases the release of
453 GABA from interneurons (Salgado et al., 2007) or elicits the activation of NMDA receptor-
454 mediated glutamatergic neurotransmission (Metherate and Hsieh, 2003; Metherate, 2004;
455 Liang et al., 2008).

456 Our finding that ACh exerts a very delicate modulation by selectively increasing
457 the evoked response to the standard sound contrasts with the gain control exerted by
458 $GABA_A$-mediated inhibition in IC (Perez-Gonzalez et al., 2012) and MGB neurons (Duque

459 et al., 2014), where the blockade of the $GABA_A$ receptors exerts a dramatic, overall
460 increase in the neural responsiveness to both deviant and standard tones (Fig. 6A,B).
461 Likewise, our finding showing that cholinergic manipulation (Fig. 3E, 4H,I) affected only
462 the steady state of the time course of adaptation, markedly contrasts with the substantial
463 changes affecting the fast- and slow decays of adaptation when the $GABA_A$ receptors were
464 blocked or activated. In agreement with our observations on the evoked response (Fig. 3A-
465 E) and FSL, a change in strength but not in latency was found to be elicited by ACh in
466 somatosensory cortical neurons (Martin-Cortecero and Nuñez, 2014). From these results,
467 we can conclude that ACh in the IC contributes to maintain the encoding of repetitive
468 acoustical input by decreasing adaptation. This occurs mainly through the activation of
469 muscarinic receptors and acts at a different time course than that of GABAergic inhibition.

470 A second difference between cholinergic and inhibitory modulation of SSA is that
471 the strength of the cholinergic effect depends on the baseline level of SSA exhibited by the
472 IC neurons (Fig 2B, 4A,B, 5B) whereas $GABA_A$-mediated inhibition affects the firing of all
473 IC neurons, regardless of the neural type, *i.e.*, adapting and non-adapting neurons (Perez-
474 Gonzalez et al., 2012). Differences in the membrane potential of the neuron and/or
475 expression of cholinergic receptors might explain the lack, modest or profound effects of
476 ACh. Thus, we suggest that neurons with partial levels of SSA filter sensory information
477 according to different cognitive states, such as attention in which ACh levels increase
478 (Passetti et al., 2000; Hasselmo and McGaughy, 2004), while neurons exhibiting extreme
479 SSA are likely to play a role as specialized filters for redundant information, *i.e.*, repetitive
480 sounds.

Although cortical SSA (Ulanovsky et al., 2003) and subcortical SSA (Malmierca et al., 2009) show many similarities, they are not the same and may play different roles (Nelken, 2014). Moreover, due to their different sources of cholinergic projections, we cannot generalize our results to ACh effects on cortical SSA. The main source of ACh to the AC is the basal forebrain (Edeline et al., 1994; Zaborszky et al., 2012; Bajo et al., 2014) while cholinergic input to the IC originates in the pontomesencephalic tegmentum (PMT, Motts and Schofield, 2009; Schofield, 2010). These different ACh sources may constitute two parallel pathways for modulating change detection in AC and IC. However it is likely that changes in cortical excitability may affect subcortical SSA by trigering the release of ACh since AC neurons inervate the PMT cholinergic neurons that project to the IC (Schofield and Motts, 2009; Schofield, 2010). Deactivation of the AC exerts a heterogeneous control on SSA in the IC (Anderson and Malmierca, 2013) that could be indirectly mediated by ACh through a disynaptic AC → PMT → IC projection. Thus, different states of cortical activation might exert a top-down control on the sensory signals being processed at IC by gating the PMT cholinergic input.

The presence of sensitive and insensitive neurons to ACh within the same IC subdivision (Fig. 5A) together with track-tracing data (Schofield, 2010; Schofield et al., 2011) and radiolabelling studies of cholinergic receptors (Rotter et al., 1979; Clarke et al., 1984; Clarke et al., 1985; Cortes and Palacios, 1986) suggest that the cholinergic projection is diffuse throughout the IC and targets specific synaptic domains populated by neurons with intermediate SSA. Alternatively, ACh may modulate specific features such as the spectral sensitivity of one type of neuron and SSA of others. Future studies are needed to address these possibilities. Here, we found that the microiontophoretic application of ACh

504 in the IC of the anesthetized rat reduces SSA which agrees with the low SSA indices
505 observed in awake animals (von der Behrens et al., 2009; Duque and Malmierca, 2014)
506 where ACh levels are higher (Kametani and Kawamura, 1990; Marrosu et al., 1995). Since
507 attention is known to increase ACh levels and neural activity (Ranganath and Rainer, 2003;
508 Deco and Thiele, 2009, 2011), our study provides a starting point to understand how
509 attention-demanding states (Passetti et al., 2000; Himmerlheber et al., 2000) might
510 modulate subcortical SSA.

511 Our finding that local augmentation of ACh increases the neural excitability (Fig.
512 3A) and attenuates adaptation to the repetitive sound (Fig. 3E) agrees with a general model
513 of how ACh affects sensory processing (reviewed in Thiele, 2013). According to this
514 model, ACh enhances the influence of feedforward afferent input relative to feedback so an
515 augmentation in ACh increase feedforward synaptic efficacy favoring information relayed
516 through the thalamus over ongoing intracortical activity. Studies in the AC (Metherate and
517 Ashe, 1993; Hsieh et al., 2000) and in other brain areas (Hasselmo and Bower, 1992;
518 Kimura, 2000; Hasselmo and McGaughy, 2004; Deco and Thiele, 2011) also support this
519 notion. Likewise, our findings support a key formulation of the predictive coding
520 framework (Friston, 2005, 2008); namely that the reduction in the neural signals evoked by
521 a repeated or predicted stimulus is attenuated by top-down processes such as attention (Kok
522 et al., 2012) or augmented by prior expectation (Todorovic et al., 2011). Recently, using
523 blocks of tone repetitions in an electroencephalographic study in humans, Moran et al.
524 (2013) found that the decreased responses to consecutive presentation of the same tone (*i.e.*,
525 repetition suppression) were markedly attenuated by systemic application of galantamine,

526 an acetylcholinesterase inhibitor. Thus, the increased availability of ACh enhances the
527 sensory representation of predicted stimuli by boosting bottom-up sensory processing.

528 In conclusion, we showed that ACh alters the sensitivity of partially-adapting IC
529 neurons by switching neural discriminability to a more linear transmission of sounds
530 (encoding most of the stimulus occurrences). This effect potentially contributes to
531 propagation of ascending sensory-evoked afferent signals through the thalamus *en route* to
532 the cortex. Our results provide empirical support for the notion that high ACh levels may
533 enhance attention to the environment, making neural circuits more responsive to external
534 sensory stimuli.

535

## LEGENDS

**Figure 1. Examples of neurons recorded in this study. A.** Dot rasters of the response to the oddball paradigm of an on-sustained neuron lacking SSA (CSI = 0.076) under baseline, ACh and recovery conditions. **B.** Time course of the Common SSA index (CSI) before, during and after the microiontophoretic injection of ACh. Neither the firing response nor the CSI were changed by the ACh application (Bootstrapping, 95% C.I.). **C.** Response of a neuron showing strong SSA (CSI = 0.974) with a distinct onset firing pattern that was unaffected by ACh (Bootstrapping, 95% C.I.). **D.** As, in B, the CSI of the strongly adapting neuron remained unchanged. **E.** Dot raster of the response of a neuron with moderate level of SSA (CSI = 0.732) that was profoundly affected by ACh showing an increase of firing rate. **F.** The CSI of this partially adapting neuron decreased during ACh injection (Bootstrapping, 95% C.I.). The tone duration (75 ms) is represented by the black bar in **A,C,E**. The duration of the ACh injection is represented by the shaded area in **B,D,F**. The small arrows in **B,D,F** indicate the times of the dot rasters displayed for each neuron.

**Figure 2. ACh effect on SSA in IC neurons. A.** The recorded IC neurons (n = 105) showed different levels of CSI in the baseline condition (○) from –0.063 to 0.994. The low and high 95% confidence interval (C.I.) of each baseline CSI is displayed (−). The CSI of a subset of IC neurons changed during the application of ACh, being higher or lower than the C.Is. of the baseline CSI value (orange symbols) while another subset of IC neurons was insensitive to ACh application (green symbols). Most of the neurons insensitive to ACh lacked SSA (CSI < 0.1) or exhibited extremely high values (CSI ≥ 0.9) in the baseline

condition (vertical histogram, left inset). Twelve neurons did not have a measurement in the recovery condition (orange and green crosses) as they were lost before full recovery. **B.** The strength of the effect of ACh depended on the baseline CSI. The baseline CSI values (○) were fitted by a Sigmoid curve ($r^2$ = 0.99, $p < 0.0001$, gray line) while the absolute difference (●, expressed in positive values) between the baseline and ACh condition followed a Gaussian curve ($r^2$ = 0.44, $p < 0.0001$, black line). **C.** Scatter plot of the difference in the frequency-specific index for f1 (SI1) and f2 (SI2) between the ACh and baseline condition ($CSI_{ACh} - CSI_{baseline}$) for neurons with low (○: CSI < 0.1), intermediate (○: 0.1 ≤ CSI < 0.9) and high CSI values (○ CSI ≥ 0.9). Each dot represents one neuron. **D.** The absolute change (positive values) in the CSI correlated similarly with the absolute changes elicited by ACh in the SI1 (Spearman´s coefficient = 0.63, $p < 0.001$) and SI2 (0.59, $p < 0.001$) indicating that changes in the response to both frequencies contributed similarly to the CSI change. Symbols with the same format as C. **E.** Box plots of the CSI (left panel) and SI1,2 (right panel) under the baseline, ACh and recovery conditions. ACh decreased the SSA indices in the population of neurons (Friedman test, *$p < 0.05$). The decrement in the SSA persisted after the spontaneous activity (SA) was subtracted to the driving response for each neuron. The dashed lines within each box represent the median values, the edges of the box delimit the 25$^{th}$ and 75$^{th}$ percentiles, the whisker bars extent to the 10$^{th}$ and 90$^{th}$ percentiles, and the circles represent the 95th and 5$^{th}$ percentiles.

**Figure 3. Effect of ACh on the driving response to deviant and standard sounds. A.** Box plot of the response to the deviant (red) and standard tone (blue) of the whole population of IC neurons (n = 105) before, during and after ACh injection, indicating that ACh increased responses to both tones (Friedman test, * $p < 0.05$). **B.** Population PSTHs

(mean ± STD, shaded) for deviant (red) and standard (blue) tones in the baseline and ACh (orange) conditions. Bin size = 1 ms; sps: spikes per second. **C.** Box plot of the firing response for those neurons with $0.1 \leq CSI < 0.9$ whose CSI was significantly affected by ACh (Bootstrapping, 95% C.I., n = 43). ACh increased only the response to the standard tone (Friedman test and Dunn's method as post hoc test, $p < 0.05$, $^*p < 0.05$). Same format as A. **D.** Population PSTHs. Same format as B. **E.** Time course of adaptation for the mean response to the standard tone for each position (trial) in the oddball sequence of neurons with $0.1 < CSI < 0.9$ significantly affected by ACh (n = 43). The baseline (●) and ACh data (●) had fast and slow decay components and a steady-state component that were fitted by a double exponential function (blue lines). ACh increased only the steady-state component. **F.** Normalized change (ACh – baseline) in the driving response (mean spikes per trial) to deviant (•) and standard tone (•) for those neurons whose CSI was changed ($CSI_{ACh} - CSI_{baseline}$) by ACh application (Bootstrapping, 95% C.I., n = 54). **G.** Normalized change in the driving response as in F but for those neurons whose CSI was not affected by ACh (Bootstrapping, 95% C.I., n = 51).

**Figure 4. Effect of scopolamine and mecamylamine on SSA. A.** The blockade of the muscarinic receptors by the application of scopolamine increased the CSI (○) in most of the recorded IC neurons. The baseline CSI values (○) were fitted by a Sigmoidal curve ($r^2 = 0.993$, $p < 0.001$, gray line). The low and high 95% bootstrapped C.I. values (−) are displayed for each baseline CSI. Similarly, the absolute differences (expressed in positive values) between the CSI in the baseline and scopolamine condition (•) were fitted by a Gaussian curve ($r^2 = 0.52$, $p = 0.003$, black line). **B.** Effect of nicotinic receptor blockade with mecamylamine. (•) Absolute differences between the CSI in the baseline and

mecamylamine condition. Same format as in A. Sigmoidal curve, $r^2 = 0.994$, $p < 0.001$; Gaussian curve, $r^2 = 0.756$, $p < 0.0001$. **C.** Box plot of the population CSI showing that scopolamine (Scop) increased the SSA as measured by the CSI (Friedman test, *$p < 0.05$, $n = 19$). **D.** Box plot of the population CSI indicating that the mecamylamine application did not affect the SSA (Friedman test, *$p > 0.05$, $n = 28$). **E.** Scatterplot of the change in the frequency-specific index ($SI_{ACh} - SI_{baseline}$) for f1 (SI1) and f2 (SI2) elicited by scopolamine (○) and mecamylamine (○). No difference between the change elicited in SI1 and SI2 by scopolamine ($p = 0.502$) and mecamylamine was found ($p = 0.33$, Mann-Whitney Rank Sum Test). **F.** Box plot of the frequency-specific index for both frequencies (SI1,2) under the baseline, scopolamine and recovery condition. Scopolamine increased the SI (Friedman, test, *$p < 0.05$, $n = 38$). **G.** Box plot of the SI1,2 indicating the lack of effect of mecamylamine (Friedman test, $p > 0.05$, $n = 56$). **H.** Mean driven response to the standard tone for each position (trial) in the oddball sequence in the baseline (•) and scopolamine conditions (•). The responses were adjusted by a double exponential function (black lines) with a fast and slow decay component and a steady-state part. Scopolamine decreased only the steady-state component. **I.** Time course of the response under the baseline (•) and scopolamine condition (•). Scopolamine did not affected the dynamics of adaptation. Same format as H.

**Figure 5. Anatomical location and physiological properties of the recorded IC neurons. A.** Box plot of the baseline CSI values in our sample of IC neurons with recording sites localized in the central nucleus (CNIC), rostral (RCIC) and lateral cortex (LCIC) of the IC. Population CSI in the RCIC and LCIC were significantly larger than CSI from the CNIC (Kruskal-Wallis test, *$p < 0.05$). CSI values affected (−) and non-affected

(−) by ACh are displayed separately. **B,C.** Effect of the ACh on the CSI of neurons from the RCIC and LCIC (B) and CNIC (C). (o) Baseline CSI with its low and high 95% bootstrapped C.I. values (−). (○) CSI value under the ACh application. (•) Absolute difference (expressed in positive values) between the CSI under the baseline and ACh condition. The change exerted by ACh on the CSI of neurons from the RCIC was fitted by a Gaussian curve ($r^2$ = 0.462, $p < 0.0001$, black line). **D.** The mean characteristic frequencies (CF) of neurons with different CSI (sorted into groups of CSI intervals of 0.1 from 0.1 to 1) were fitted by a linear function ($r^2$ = 0.533, p = 0.016, black line) indicating that neurons with low CSI are tuned to lower frequencies than those neurons with higher CSI. **E.** The duration of the driving response of IC neurons with different CSI (sorted into groups of CSI intervals of 0.1 from 0.1 to 1) were fitted by a linear function ($r^2$ = 0.526, p = 0.017, black line) indicating that neurons with higher CSI exhibited shorter responses than those neurons with higher CSI.

**Figure 6. Schematic diagram of the acetylcholine effect (and gabazine for comparison purposes) on the response (firing rate) and dynamics of adaptation (time course of adaptation). A.** The microiontophoretic application of acetylcholine decreased the CSI by selectively increasing the responses to the standard tone (blue) alone. Note that the response to the deviant tone is virtually unaffected (red). **B**. The blockade of the $GABA_A$ receptors using the microiontophoretic application of gabazine decreased the CSI by increasing *both*, the response to the standard (blue) and deviant sound (red) as demonstrated by Perez-Gonzalez et al., 2012. **C.** The time course of adaptation of the response to the standard tone is affected differently by gabazine and acetylcholine. Gabazine increased the three

components of adaptation, *i.e.*, the fast and slow decay as well as the sustained component of adaptation while the acetylcholine increased the sustained component only.

## REFERENCES


Abolafia JM, Vergara R, Arnold MM, Reig R, Sanchez-Vives MV (2011) Cortical auditory adaptation in the awake rat and the role of potassium currents. Cereb Cortex 21:977-990.

Anderson LA, Malmierca MS (2012) The effect of auditory cortex deactivation on stimulus-specific adaptation in the inferior colliculus of the rat. Eur J Neurosci 37:52-62.

Antunes FM, Nelken I, Covey E, Malmierca MS (2010) Stimulus-specific adaptation in the auditory thalamus of the anesthetized rat. PLoS One 5:e14071.

Ashe, J. H., McKenna, T. M., & Weinberger, N. M. (1989). Cholinergic modulation of frequency receptive fields in auditory cortex: II. Frequency-specific effects of anticholinesterases provide evidence for a modulatory action of endogenous ACh. Synapse, 4(1), 44–54.

Ayala YA, Malmierca MS (2013) Stimulus-specific adaptation and deviance detection in the inferior colliculus. Front Neural Circuits 6:89.

Ayala YA, Malmierca MS (2014) Cholinergic modulation of stimulus-specific adaptation in the inferior colliculus. FENS-0809. 9th FENS Forum of Neuroscience. Milan. Italy.

Ayala YA, Malmierca MS (2015) Modulation of auditory deviant saliency in the inferior collisulus. PS-430. ARO MidWinter Meeting. Baltimore. USA.

Ayala YA, Udeh A, Dutta K, Bishop D, Malmierca MS, Oliver DL (2015) Differences in the strength of cortical and brainstem inputs to SSA and non-SSA neurons in the inferior colliculus. Scientific Rep. *In press.*

676 Ayala YA, Perez-Gonzalez D, Duque D, Nelken I, Malmierca MS (2013) Frequency
677 discrimination and stimulus deviance in the inferior colliculus and cochlear nucleus.
678 Front Neural Circuits 6:119.
679 Bajo VM, Leach ND, Cordery PM, Nodal FR, King AJ (2014) The cholinergic basal
680 forebrain in the ferret and its inputs to the auditory cortex. Eur J Neurosci 40:2922-
681 2940.
682 Barkai E, Hasselmo ME (1994) Modulation of the input/output function of rat piriform
683 cortex pyramidal cells. J Neurophysiol 72:644-658.
684 Boucetta S, Jones BE (2009) Activity profiles of cholinergic and intermingled GABAergic
685 and putative glutamatergic neurons in the pontomesencephalic tegmentum of
686 urethane-anesthetized rats. J Neurosci 29:4664-4674.
687 Clarke PB, Pert CB, Pert A (1984) Autoradiographic distribution of nicotine receptors in rat
688 brain. Brain Res 323:390-395.
689 Clarke PB, Schwartz RD, Paul SM, Pert CB, Pert A (1985) Nicotinic binding in rat brain:
690 autoradiographic comparison of [3H]acetylcholine, [3H]nicotine, and [125I]-alpha-
691 bungarotoxin. J Neurosci 5:1307-1315.
692 Cole AE, Nicoll RA (1984) The pharmacology of cholinergic excitatory responses in
693 hippocampal pyramidal cells. Brain Res 305:283-290.
694 Cortes R, Palacios JM (1986) Muscarinic cholinergic receptor subtypes in the rat brain. I.
695 Quantitative autoradiographic studies. Brain Res 362:227-238.
696 Deco G, Thiele A (2009) Attention: oscillations and neuropharmacology. Eur J Neurosci
697 30:347-354.

698 Deco G, Thiele A (2011) Cholinergic control of cortical network interactions enables
699 feedback-mediated attentional modulation. Eur J Neurosci 34:146-157.
700 Disney AA, Aoki C, Hawken MJ (2007) Gain modulation by nicotine in macaque v1.
701 Neuron 56:701-713.
702 Disney AA, Aoki C, Hawken MJ (2012) Cholinergic suppression of visual responses in
703 primate V1 is mediated by GABAergic inhibition. J Neurophysiol 108:1907-1923.
704 Duque D, Malmierca MS (2014) Stimulus-specific adaptation in the inferior colliculus of
705 the mouse: anesthesia and spontaneous activity effects. Brain Struct Funct.
706 Edeline JM, Hars B, Maho C, Hennevin E (1994) Transient and prolonged facilitation of
707 tone-evoked responses induced by basal forebrain stimulations in the rat auditory
708 cortex. Exp Brain Res 97:373-386.
709 Escera C, Malmierca MS (2014) The auditory novelty system: an attempt to integrate
710 human and animal research. Psychophysiology 51:111-123
711 Farley BJ, Quirk MC, Doherty JJ, Christian EP (2010) Stimulus-specific adaptation in
712 auditory cortex is an NMDA-independent process distinct from the sensory novelty
713 encoded by the mismatch negativity. J Neurosci 30:16475-16484.
714 Farley GR, Morley BJ, Javel E, Gorga MP (1983) Single-unit responses to cholinergic
715 agents in the rat inferior colliculus. Hear Res 11:73-91.
716 Faure PA, Fremouw T, Casseday JH, Covey E (2003) Temporal masking reveals properties
717 of sound-evoked inhibition in duration-tuned neurons of the inferior colliculus. J
718 Neurosci 23:3052-3065.

719 Flores-Hernandez J, Salgado H, De La Rosa V, Avila-Ruiz T, Torres-Ramirez O, Lopez-
720 Lopez G, Atzori M (2009) Cholinergic direct inhibition of N-methyl-D aspartate
721 receptor-mediated currents in the rat neocortex. Synapse 63:308-318.
722 Friston K (2005) A theory of cortical responses. Philos Trans R Soc Lond B Biol Sci
723 360:815-836.
724 Friston K (2008) Hierarchical models in the brain. PLoS Comput Biol 4:e1000211.
725 Froemke RC, Merzenich MM, Schreiner CE (2007) A synaptic memory trace for cortical
726 receptive field plasticity. Nature 450:425-429.
727 Garcia-Rill E (1991) The pedunculopontine nucleus. Prog Neurobiol 36:363-389.
728 Goldstein-Daruech N, Pedemonte M, Inderkum A, Velluti RA (2002) Effects of excitatory
729 amino acid antagonists on the activity of inferior colliculus neurons during sleep
730 and wakefulness. Hear Res 168:174-180.
731 Grimm S, Escera C (2012) Auditory deviance detection revisited: evidence for a
732 hierarchical novelty system. Int J Psychophysiol 85:88-92
733 Grupe M, Grunnet M, Laursen B, Bastlund, JF (2013) Neuropharmacol ogical modulation
734 of the P3-like event-related potential in a rat two-tone auditory discrimin ation task
735 with modafinil and NS9283, a positive allosteric modulator of a4b2 nAChRs J
736 Neuropharm 79: 444-455.
737 Habbicht H, Vater M (1996) A microiontophoretic study of acetylcholine effects in the
738 inferior colliculus of horseshoe bats: implications for a modulatory role. Brain Res
739 724:169-179.
740 Hasselmo ME, Bower JM (1992) Cholinergic suppression specific to intrinsic not afferent
741 fiber synapses in rat piriform (olfactory) cortex. J Neurophysiol 67:1222-1229.

742 Hasselmo ME, McGaughy J (2004) High acetylcholine levels set circuit dynamics for
743 attention and encoding and low acetylcholine levels set dynamics for consolidation.
744 Prog Brain Res 145:207-231.
745 Havey DC, Caspary DM (1980) A simple technique for constructing 'piggy-back'
746 multibarrel microelectrodes. Electroencephalogr Clin Neurophysiol 48: 249-251
747 Hernandez O, Espinosa N, Perez-Gonzalez D, Malmierca MS (2005) The inferior colliculus
748 of the rat: a quantitative analysis of monaural frequency response areas.
749 Neuroscience 132:203-217.
750 Himmelheber, A., Sarter, M. and Bruno, J. (2000) Increases in cortical acetylcholine
751 release during sustained attention performance in rats. Cognitive Brain Research, 9:
752 313–325.
753 Hsieh CY, Cruikshank SJ, Metherate R (2000) Differential modulation of auditory
754 thalamocortical and intracortical synaptic transmission by cholinergic agonist. Brain
755 Res 880:51-64.
756 Ji W, Gao E, Suga N (2001) Effects of acetylcholine and atropine on plasticity of central
757 auditory neurons caused by conditioning in bats. J Neurophysiol 86:211-225.
758 Jones BE (2008) Modulation of cortical activation and behavioral arousal by cholinergic
759 and orexinergic systems. Ann N Y Acad Sci 1129:26-34.
760 Kametani, H. and Kawamura, H. (1990) Alterations in
761 acetylcholine release in the rat hippocampus during sleep wakefulness detected by
762 intracerebral dialysis. Life Sci., 47: 421–426.
763 Kelly JB, Caspary DM (2005) Pharmacology of the inferior colliculus. In: The Inferior
764 Colliculus (Winer JA, Schreiner CE, eds), pp 248-281. New York: Springer.

765 Kiebel SJ, Daunizeau J, Friston KJ (2009) Perception and hierarchical dynamics. Front
766 Neuroinform 3:20.
767 Kimura F (2000) Cholinergic modulation of cortical function: a hypothetical role in shifting
768 the dynamics in cortical network. Neurosci Res 38:19-26.
769 Knott V, Impey D, Philippe T, Smith D, Choueiry J, de la Salle S, Dort H (2014)
770 Modulation of auditory deviance detection by acute nicotine is baseline and deviant
771 dependent in healthy nonsmokers: a mismatch negativity study. Hum
772 Psychopharmacol 29:446-458.
773 Kok P, Rahnev D, Jehee JF, Lau HC, de Lange FP (2012). Attention reverses the effect of
774 prediction in silencing sensory signals. Cereb Cortex 22:2197-2206.
775 Krause M, Pedarzani P (2000) A protein phosphatase is involved in the cholinergic
776 suppression of the Ca(2+)-activated K(+) current sI(AHP) in hippocampal
777 pyramidal neurons. Neuropharmacology 39:1274-1283.
778 Krnjevic K (2004) Synaptic mechanisms modulated by acetylcholine in cerebral cortex.
779 Prog Brain Res 145:81-93.
780 Kruglikov I, Rudy B (2008) Perisomatic GABA release and thalamocortical integration
781 onto neocortical excitatory cells are regulated by neuromodulators. Neuron 58:911-
782 924.
783 LeBeau FE, Malmierca MS, Rees A (2001) Iontophoresis in vivo demonstrates a key role
784 for GABA(A) and glycinergic inhibition in shaping frequency response areas in the
785 inferior colliculus of guinea pig. J Neurosci 21:7303-7312.

786 Levy RB, Aoki C (2002) Alpha7 nicotinic acetylcholine receptors occur at postsynaptic
787 densities of AMPA receptor-positive and -negative excitatory synapses in rat
788 sensory cortex. J Neurosci 22:5001-5015.
789 Liang K, Poytress BS, Weinberger NM, Metherate R (2008) Nicotinic modulation of tone-
790 evoked responses in auditory cortex reflects the strength of prior auditory learning.
791 Neurobiol Learn Mem 90:138-146.
792 Loftus WC, Malmierca MS, Bishop DC, Oliver DL (2008) The cytoarchitecture of the
793 inferior colliculus revisited: a common organization of the lateral cortex in rat and
794 cat. Neuroscience 12:196-205.
795 Lumani A, Zhang H (2010) Responses of neurons in the rat's dorsal cortex of the inferior
796 colliculus to monaural tone bursts. Brain Res 1351:115-129.
797 Malmierca MS, Cristaudo S, Perez-Gonzalez D, Covey E (2009) Stimulus-specific
798 adaptation in the inferior colliculus of the anesthetized rat. J Neurosci 29:5483-
799 5493.
800 Malmierca MS, Sanchez-Vives MV, Escera C, Bendixen A (2014) Neuronal adaptation,
801 novelty detection and regularity encoding in audition. Front Syst Neurosci 8:111.
802 Martin-Cortecero J, Nunez A (2014) Tactile response adaptation to whisker stimulation in
803 the lemniscal somatosensory pathway of rats. Brain Res 1591C:27-37.
804 Marrosu, F., Portas, C., Mascia, M.S., Casu, M.A., Fa, M., Giagheddu, M., Imperato, A.
805 and Gessa, G.L. (1995) Microdialysis measurement of cortical and hippocampal
806 acetylcholine release during sleep-wake cycle in freely moving cats. Brain Res.,
807 671: 329–332

McCormick DA (1993) Actions of acetylcholine in the cerebral cortex and thalamus and implications for function. Prog Brain Res 98:303-308.

McCormick DA, Prince DA (1986) Acetylcholine induces burst firing in thalamic reticular neurones by activating a potassium conductance. Nature 319:402-405.

Ma, X., & Suga, N. (2005). Long-term cortical plasticity evoked by electric stimulation and acetylcholine applied to the auditory cortex. Proceedings of the National Academy of Sciences of the United States of America, 102(26), 9335–9340.

Malmierca MS, Hernandez O, Falconi A, Lopez-Poveda EA, Merchan M, Rees A (2003) The commissure of the inferior colliculus shapes frequency response areas in rat: an in vivo study using reversible blockade with microinjection of kynurenic acid. Exp Brain Res 153:522-529.

Malmierca MS, Izquierdo MA, Cristaudo S, Hernandez O, Perez-Gonzalez D, Covey E, Oliver DL (2008) A discontinuous tonotopic organization in the inferior colliculus of the rat. J Neurosci 28:4767-4776.

Malmierca MS, Sanchez-Vives MV, Escera C, Bendixen A (2014) Neuronal adaptation, novelty detection and regularity encoding in audition. Front Syst Neurosci, 8:111. doi:10.3389/fnsys.2014.00111

Merrill EG, Ainsworth A (1972) Glass-coated platinum coated tungsten microelectrodes. Med Biol Eng 10:662– 672.

Metherate R (2004) Nicotinic acetylcholine receptors in sensory cortex. Learn Mem 11:50-59.

829 Metherate R (2011) Functional connectivity and cholinergic modulation in auditory cortex.
830 Neurosci Biobehav Rev 35:2058-2063.
831 Metherate R, Ashe JH (1993) Nucleus basalis stimulation facilitates thalamocortical
832 synaptic transmission in the rat auditory cortex. Synapse 14:132-143.
833 Metherate R, Hsieh CY (2003) Regulation of glutamate synapses by nicotinic acetylcholine
834 receptors in auditory cortex. Neurobiol Learn Mem 80:285-290.
835 Metherate R, Weinberger NM (1989) Acetylcholine produces stimulus-specific receptive
836 field alterations in cat auditory cortex. Brain Res 480:372-377.
837 Metherate, R. and Weinberger, N.M. (1990) Cholinergic modulation of responses to single
838 tones produces tone-specific receptive-field alterations in cat auditory-cortex.
839 Synapse 6: 133–145.
840 Metherate, R., Ashe, J.H. and Weinberger, N.M. (1990) Acetylcholine modifies neuronal
841 acoustic rate level functions in guinea pig auditory cortex by an action at muscarinic
842 receptors. Synapse 6: 364–368.
843 Metherate R, Cox CL, Ashe JH (1992) Cellular bases of neocortical activation: modulation
844 of neural oscillations by the nucleus basalis and endogenous acetylcholine. J
845 Neurosci 12:4701-4711.
846 Moran RJ, Campo P, Symmonds M, Stephan KE, Dolan RJ, Friston KJ (2013) Free energy,
847 precision and learning: the role of cholinergic neuromodulation. J Neurosci
848 33:8227-8236.
849 Morley BJ, Kemp GE (1981) Characterization of a putative nicotinic acetylcholine receptor
850 in mammalian brain. Brain Res 228:81-104.

851 Motts SD, Schofield BR (2009) Sources of cholinergic input to the inferior colliculus.
852 Neuroscience 160:103-114.
853 Näätänen R (1992) Attention and brain function. Hillsdale, NJ: Lawrence Erlbaum.
854 Nelken I, Ulanovsky N (2007) Mismatch negativity and simulus-specific adaptation in
855 animal models. J Psychophysiol 21:214 –223.
856 Nelken I (2014) Stimulus-specific adaptation and deviance detection in the auditory
857 system: experiments and models. Biol Cybern doi:10.1007/s00422-014-0585-7
858 Passetti F, Dalley JW, O'Connell MT, Everitt BJ, Robbins TW (2000) Increased
859 acetylcholine release in the rat medial prefrontal cortex during performance of a
860 visual attentional task. Eur J Neurosci 12:3051-3058.
861 Paxinos G, Watson C (2005) The rat brain in stereotaxic coordinates. Burlington, VT:
862 Elsevier-Academic.
863 Pérez-González D, Malmierca MS, Covey E (2005) Novelty detector neurons in the
864 mammalian auditory midbrain. Eur J Neurosci 22:2879-2885.
865 Perez-Gonzalez D, Hernandez O, Covey E, Malmierca MS (2012) GABA(A)-Mediated
866 Inhibition Modulates Stimulus-Specific Adaptation in the Inferior Colliculus. PLoS
867 One 7:e34297.
868 Picciotto MR, Higley MJ, Mineur YS (2012). Acetylcholine as a neuromodulator:
869 cholinergic signaling shapes nervous system function and behavior. Neuron 76:116-
870 129.
871 Poorthuis RB, Goriounova NA, Couey JJ, Mansvelder HD (2009) Nicotinic actions on
872 neuronal networks for cognition: general principles and long-term consequences.
873 Biochem Pharmacol 78:668-676.

874 Ranganath C, Rainer G (2003) Neural mechanisms for detecting and remembering novel
875 events. Nat Rev Neurosci 4:193-202.
876 Rees A (1990) A close-field sound system for auditory neurophysiology. J of Physiol
877 430:2.
878 Rees A, Sarbaz A, Malmierca MS, Le Beau FE (1997) Regularity of firing of neurons in
879 the inferior colliculus. J Neurophysiol 77:2945-2965.
880 Richardson BD, Hancock KE, Caspary DM (2013) Stimulus-specific adaptation in auditory
881 thalamus of young and aged awake rats. J Neurophysiol 110:1892-1902.
882 Rotter A, Birdsall NJ, Field PM, Raisman G (1979) Muscarinic receptors in the central
883 nervous system of the rat. II. Distribution of binding of [3H]propylbenzilylcholine
884 mustard in the midbrain and hindbrain. Brain Res 180:167-183.
885 Salgado H, Bellay T, Nichols JA, Bose M, Martinolich L, Perrotti L, Atzori M (2007)
886 Muscarinic M2 and M1 receptors reduce GABA release by Ca2+ channel
887 modulation through activation of PI3K/Ca2+ -independent and PLC/Ca2+ -
888 dependent PKC. J Neurophysiol 98:952-965.
889 Sanchez-Vives, M. V., Nowak, L. G., and McCormick, D. A. (2000a). Cellular
890 mechanisms of long-lasting adaptation in visual cortical neurons in vitro.
891 J. Neurosci. 20, 4286–4299.
892 Sanchez-Vives, M. V., Nowak, L. G., and McCormick, D. A. (2000b). Membrane
893 mechanisms underlying contrast adaptation in cat area 17 in vivo. J. Neurosci.
894 20, 4267–4285.

895 Sarter M, Hasselmo ME, Bruno JP, Givens B (2005) Unraveling the attentional functions
896 of cortical cholinergic inputs: interactions between signal-driven and cognitive
897 modulation of signal detection. Brain Res Rev 48:98–111. CrossRef Medline
898 Schofield BR (2010) Projections from auditory cortex to midbrain cholinergic neurons that
899 project to the inferior colliculus. Neuroscience 166:231-240.
900 Schofield BR, Motts SD (2009) Projections from auditory cortex to cholinergic cells in the
901 midbrain tegmentum of guinea pigs. Brain Res Bull 80:163-170.
902 Schofield BR, Motts SD, Mellott JG (2011) Cholinergic cells of the pontomesencephalic
903 tegmentum: connections with auditory structures from cochlear nucleus to cortex.
904 Hear Res 279:85-95.
905 Steriade M, Pare D, Parent A, Smith Y (1988) Projections of cholinergic and non-
906 cholinergic neurons of the brainstem core to relay and associational thalamic nuclei
907 in the cat and macaque monkey. Neuroscience 25:47-67.
908 Thiele A (2013) Muscarinic signaling in the brain. Annu Rev Neurosci 36:271-294.
909 Thiel CM, Fink GR (2008) Effects of the cholinergic agonist nicotine on reorienting of
910 visual spatial attention and top-down attentional control. Neuroscience 152:381–
911 390.
912 Todorovic A, van Ede F, Maris E, de Lange FP (2011) Prior expectation mediates neural
913 adaptation to repeated sound in the auditory cortex: an MEG study. J Neurosc 31:
914 9118-9123.
915 von der Behrens W, Bauerle P, Kossl M, Gaese BH (2009) Correlating stimulus-specific
916 adaptation of cortical neurons and local field potentials in the awake rat. J Neurosci
917 29:13837-13849.

Watanabe T, Simada Z (1973) Pharmacological properties of cat's collicular auditory neurons. Jpn J Physiol 23:291-308.

Watkins PV, Barbour DL (2011) Level-tuned neurons in primary auditory cortex adapt differently to loud versus soft sounds. Cereb Cortex 21:178-190.

Zaborszky L, Van den A, Gyengesi E (2012) The basal forebrain cholinergic projection system in mice. In: Watson C, Paxinos G, Puelles L, editors. The mouse nervous system. 1st ed. Amsterdam: Elsevier. p. 684-718.

Zhang W, Yamada M, Gomeza J, Basile AS, Wess J (2002) Multiple muscarinic acetylcholine receptor subtypes modulate striatal dopamine release, as studied with M1-M5 muscarinic receptor knock-out mice. J Neurosci 22:6347-6352.

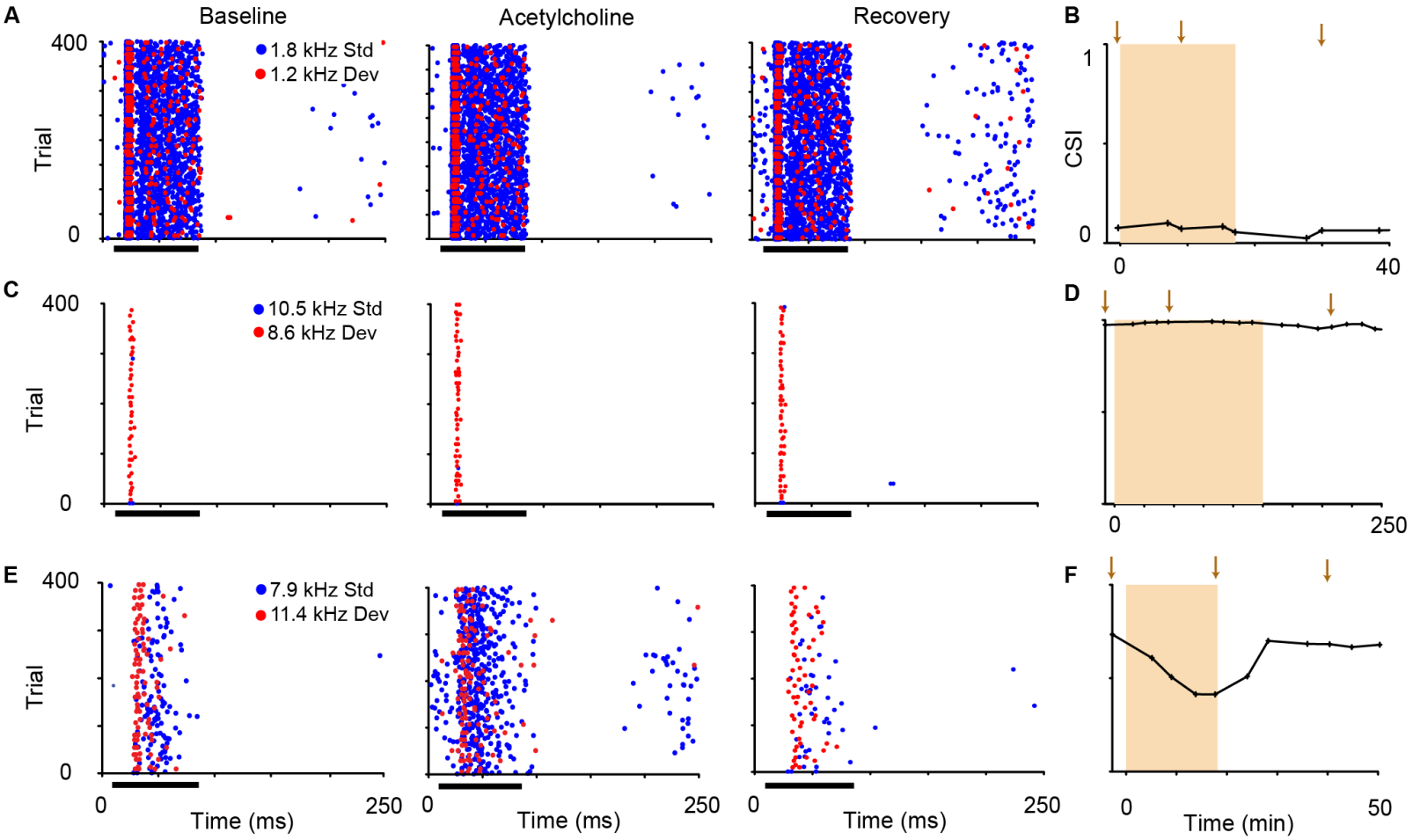
A
Baseline
Acetylcholine
Recovery
400
0
Trial
1.8 kHz Std
1.2 kHz Dev
B
1
0
CSI
0
40
C
400
0
Trial
10.5 kHz Std
8.6 kHz Dev
D
0
250
E
400
0
Trial
7.9 kHz Std
11.4 kHz Dev
0
250
Time (ms)
0
250
Time (ms)
0
250
Time (ms)
F
0
50
Time (min)

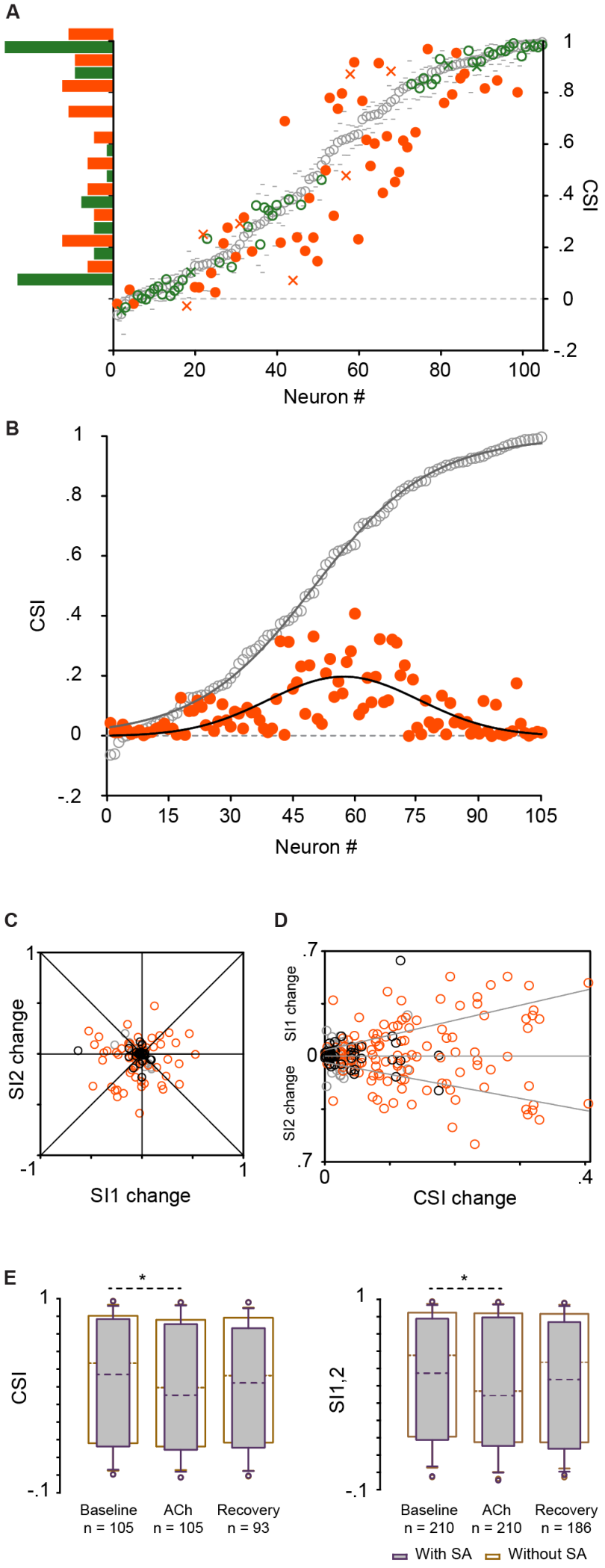
A
1
.8
.6
.4
.2
0
-.2
CSI
0
20
40
60
80
100
Neuron #
B
1
.8
.6
.4
.2
0
-.2
CSI
0
15
30
45
60
75
90
105
Neuron #
C
1
-1
1
SI2 change
SI1 change
D
.7
0
.7
SI1 change
SI2 change
0
.4
CSI change
E
1
-.1
CSI
*
Baseline
n = 105
ACh
n = 105
Recovery
n = 93
1
-.1
SI1,2
*
Baseline
n = 210
ACh
n = 210
Recovery
n = 186
With SA
Without SA

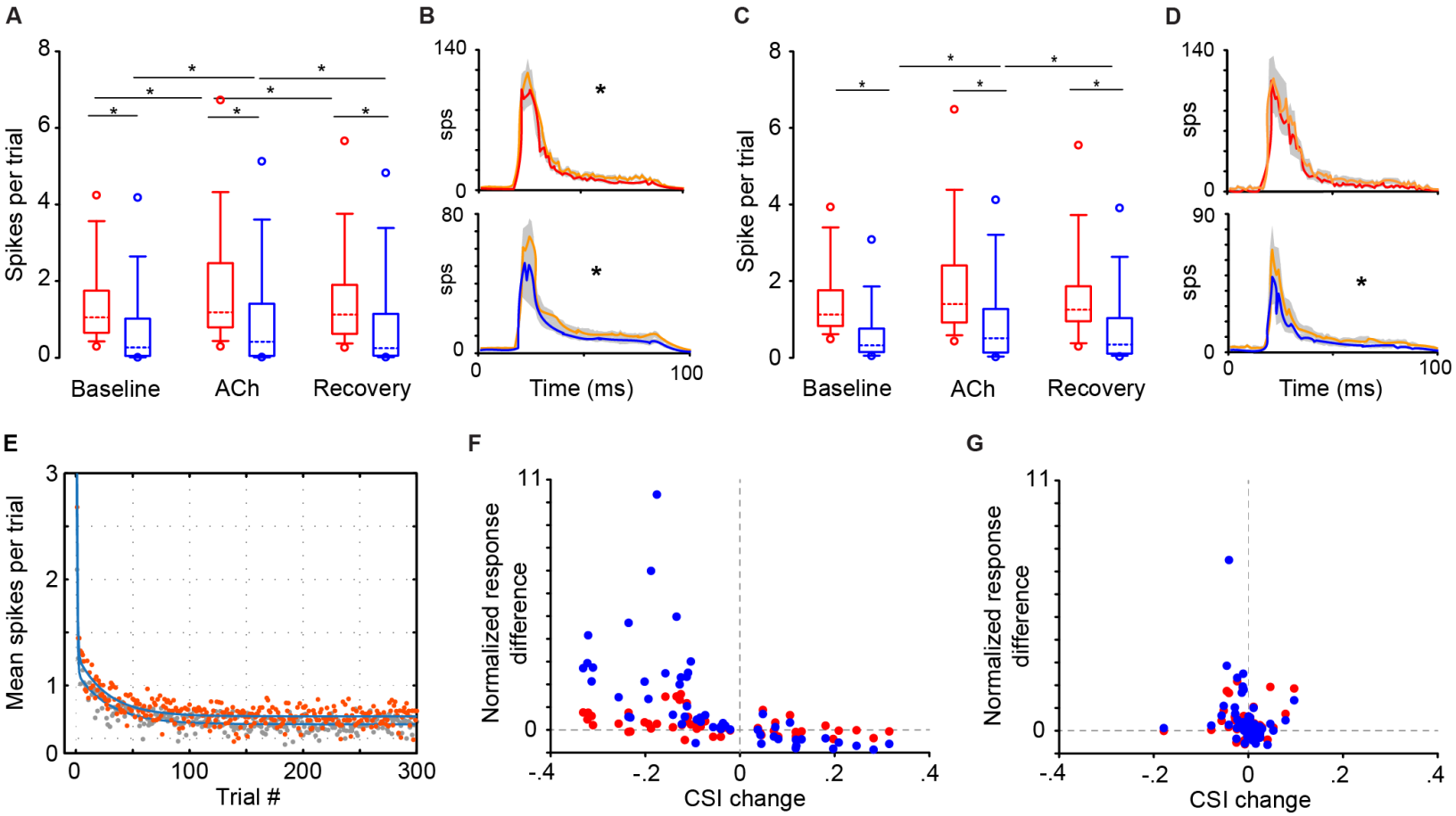
A
B
C
D
Spikes per trial
Spike per trial
Baseline
ACh
Recovery
sps
Time (ms)
E
F
G
Mean spikes per trial
Trial #
Normalized response difference
CSI change

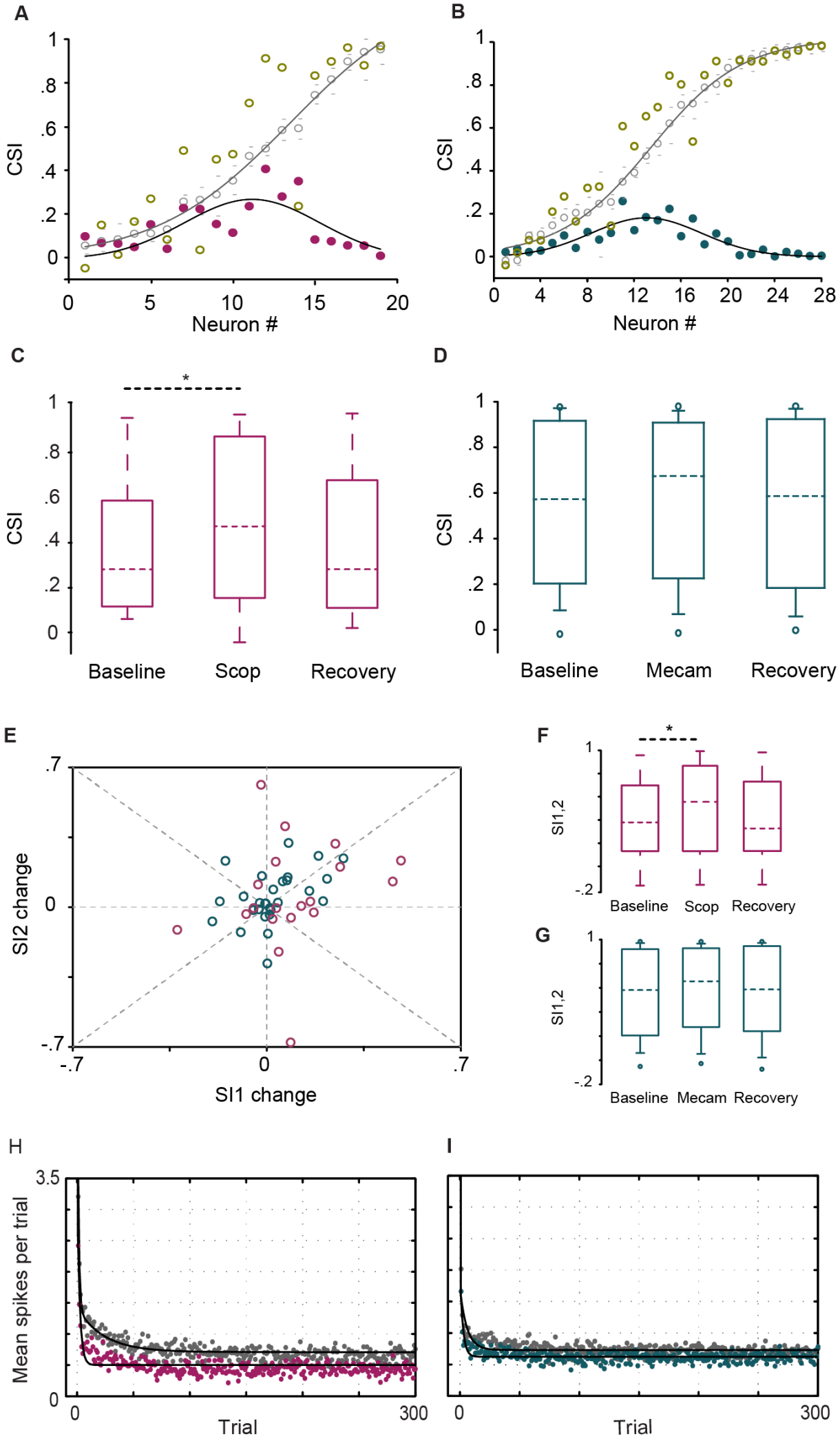
A
B
CSI
Neuron #
C
D
*
Baseline
Scop
Recovery
Mecam
E
SI2 change
SI1 change
F
G
SI1,2
H
I
Mean spikes per trial
Trial

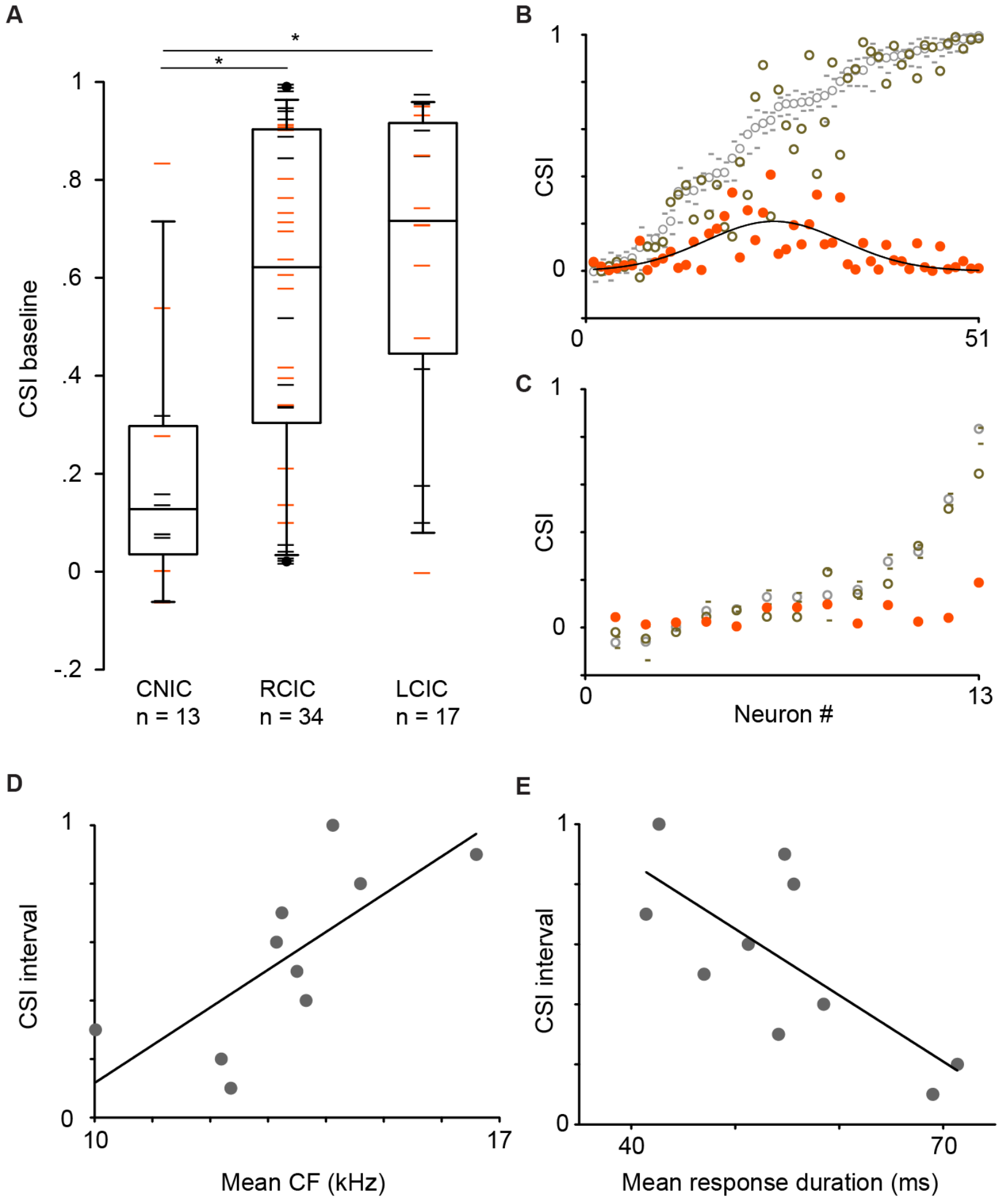
A
B
C
D
E
CSI baseline
1
.8
.6
.4
.2
0
-.2
*
*
CNIC
n = 13
RCIC
n = 34
LCIC
n = 17
CSI
1
0
0
51
CSI
1
0
0
13
Neuron #
CSI interval
1
0
10
17
Mean CF (kHz)
CSI interval
1
0
40
70
Mean response duration (ms)

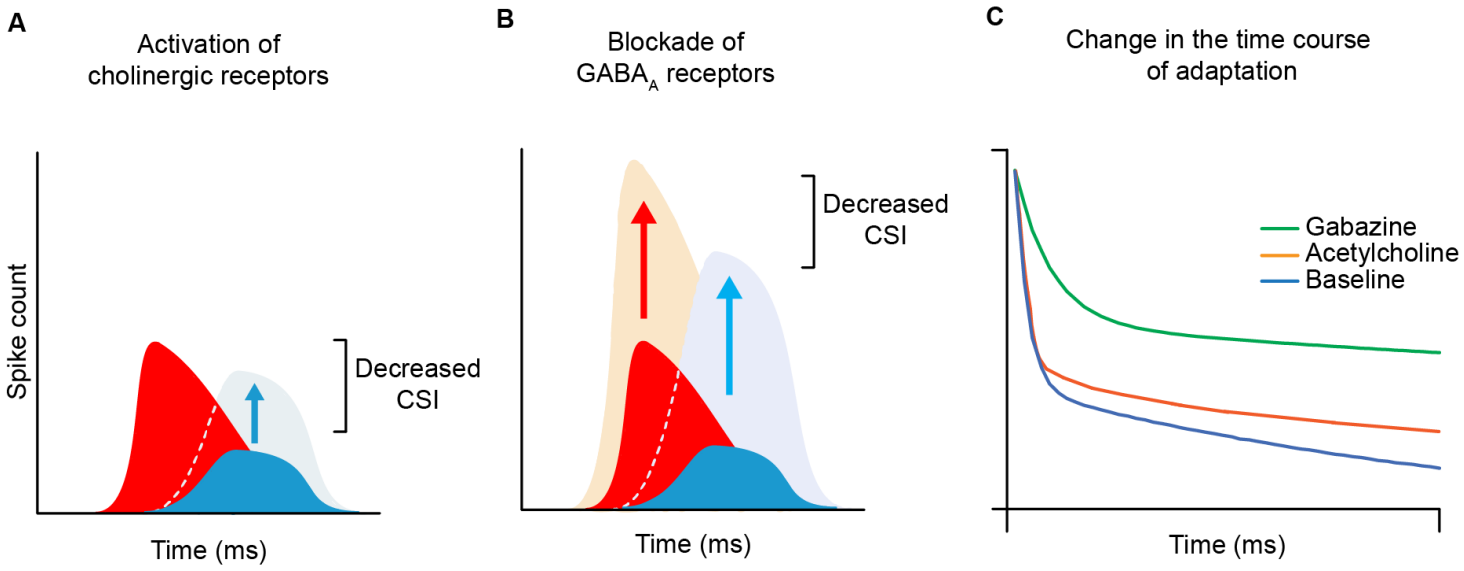
A
Activation of
cholinergic receptors
Spike count
Decreased
CSI
Time (ms)
B
Blockade of
GABA$_A$ receptors
Decreased
CSI
Time (ms)
C
Change in the time course
of adaptation
Gabazine
Acetylcholine
Baseline
Time (ms)